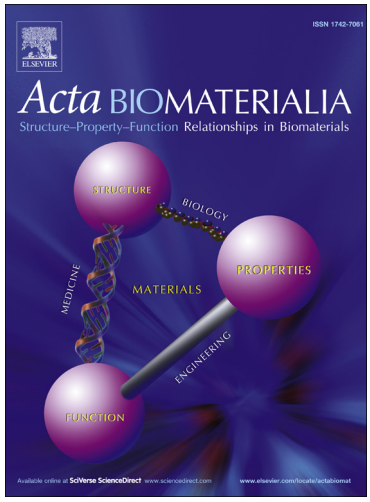

Shape-memory porous alginate scaffolds for regeneration of the annulus fibrosus - Effect of TGF-β3 supplementation and oxygen culture conditions

Olivier Guillaume, Andrew Daly, Kerri Lennon, Jennifer Gansau, Shane F. Buckley, Conor T. Buckley

PII: S1742-7061(13)00642-9
DOI: http://dx.doi.org/10.1016/j.actbio.2013.12.037
Reference: ACTBIO 3041

To appear in: *Acta Biomaterialia*

Received Date: 21 August 2013
Revised Date: 16 December 2013
Accepted Date: 19 December 2013

Please cite this article as: Guillaume, O., Daly, A., Lennon, K., Gansau, J., Buckley, S.F., Buckley, C.T., Shape-memory porous alginate scaffolds for regeneration of the annulus fibrosus - Effect of TGF-β3 supplementation and oxygen culture conditions, *Acta Biomaterialia* (2013), doi: http://dx.doi.org/10.1016/j.actbio.2013.12.037

Shape-memory porous alginate scaffolds for regeneration of the annulus fibrosus - Effect of TGF-β3 supplementation and oxygen culture conditions

Olivier Guillaume [1,2], Andrew Daly[1,2], Kerri Lennon[1,2], Jennifer Gansau[1,2], Shane F. Buckley [1,2] and Conor T. Buckley [1,2*]

[1] Trinity Centre for Bioengineering, Trinity Biomedical Sciences Institute, Trinity College Dublin, Ireland.

[2] Department of Mechanical Engineering, School of Engineering, Trinity College Dublin, Ireland.

*Corresponding author: Conor T. Buckley

E-mail address: conor.buckley@tcd.ie

Address: Trinity Centre for Bioengineering

Trinity Biomedical Sciences Institute

Trinity College Dublin

Ireland

Telephone: +353-1-896-2061

Fax: +353-1-679-5554

Abstract

Disc herniation as a result of degenerative or traumatic injury is believed to be the primary instigator of low back pain. At present there is a lack of viable treatment options to repair damaged annulus fibrosus tissue (AF). Developing alternative strategies to fill and repair ruptured AF tissue is a key challenge.

In this work we developed a porous alginate scaffold with shape-memory properties which can be delivered using minimally invasive approaches and recover its original geometry once hydrated. Covalently cross-linked alginate hydrogels were created using carbodiimide chemistry, followed by a freeze-drying step to impart porosity and create porous scaffolds. Results showed that porous alginate scaffolds exhibited shape-memory recovery and mechanical behaviour that could be modulated depending on the cross-linker concentrations. The scaffold can be repeatedly compressed and expanded, which provides the potential to deliver the biomaterial directly to the damaged area of the AF tissue. *In vitro* experiments demonstrated that scaffolds were cytocompatible and supported cell seeding, penetration and proliferation under IVD-like microenvironmental conditions (low glucose media and low oxygen concentration). Extra-cellular matrix (ECM) was secreted by AF cells with TGF-β3 stimulation and after 21 days had filled the porous scaffold network. This biological matrix was rich in sulphated-glycosaminoglycan and collagen type I, which are the main compounds of native AF tissue. Successful ECM deposition was also confirmed by the increase in the peak stress of the scaffold. However, the immaturity of the matrix network after only 21 days of *in vitro* culture was not sufficient to attain native AF tissue mechanical properties.

The ability to deliver porous scaffolds using minimal invasive approaches that can potentially promote the regeneration of AF defects provides an exciting new avenue for disc repair.

Key words: Shape-memory, scaffold, alginate, annulus fibrosus, intervertebral disc.

1. Introduction

The intervertebral disc (IVD), which lies between each vertebra of the backbone, is a complex structure composed of a gelatinous-like tissue in the core (the nucleus pulposus, NP) enclosed by the annulus fibrosus tissue (AF). The NP is rich in sulphated-glycosaminoglycan (sGAG) and collagen type II and maintains daily compressive loads due to its high hydration. The AF is mainly composed of organized lamella of collagen (collagen type I) anchored to the vertebra and its function is to radially restrain the NP in the centre of the IVD [1].

However, due to injury or degeneration, tears or fissures can occur in the AF tissue through which the soft gelatinous NP tissue can protrude and impinge on nerve roots resulting in low back pain (LBP) and reduced disc height [2, 3]. Current surgical interventions include discectomy or in severe cases spinal fusion, which alleviate pain but do not restore disc functionality [4, 5]. For example, in 2011 the US patient population suffering from LBP was estimated to be around 5 million and required 500 000 lumbar fusion or discectomy procedures to be performed [6]. After discectomy, recurrent herniations and LBP are commonly experienced by the patient, and may partially be attributed to the non-complete healing of the damaged AF. Specifically after surgical discectomy, approximately 10 to 25% of patients experienced moderate to severe chronic pain, which is identified to be a direct consequence of annular fissures [7].

Attempts to close the defect in the AF using closure devices have been undertaken and some implants are commercially available (*i.e.* suture with anchorage system (X-close® by Anulex [8]) or implant (Barricaid® from Intrinsic Therapeutics [9]) but without having demonstrated strong evidence of long term safety and efficacy [10-12]. More importantly,

these devices primarily act as a barrier aimed at sealing the defect and preventing the NP from exiting through the AF. However, their use is perhaps limited by their inability to integrate and promote biological repair of the AF tissue and, finally, to prevent further degeneration. Considerable efforts have been made in IVD regeneration using tissue engineering strategies with research mainly targeting repair of the nucleus pulposus [13, 14], and the need for new strategies for AF regeneration has only recently emerged. Developing biomaterial-based strategies to seal, promote biological repair and integration of ruptured annulus fibrosus is of significant importance and a key challenge. Ideally any biomaterial intended to be used for the regeneration of the AF tissue should be biocompatible, biodegradable, able to quickly fill defects or fissures of any shape and have the capacity to stimulate tissue regeneration post-implantation [10]. Several attempts have been made using tissue engineering strategies, including porous scaffolds [15-17] or fibrous constructs [18, 19], of natural [16, 20, 21] or synthetic biomaterials [15, 17]. Nevertheless, one major parameter which has been overlooked so far is the deliverability of these biomaterials.

Developing a porous scaffold which could be delivered directly to AF defects of the IVD using minimally invasive surgery (MIS) could be appealing for both the surgeon and the patient. The attractiveness of MIS compared to traditional open-procedure surgeries results in less post-surgical complications (*e.g.* infection, bleeding, pain at the site graft), in greater comfort for the patient, reduced hospital stay, rehabilitation and healthcare costs [22, 23].

The IVD microenvironment is characterized by low pH, high lactate concentration, low serum, low glucose and low oxygen concentration, which evolve during degeneration phases [24-26]. Such parameters have been shown to significantly influence disc cell behaviour [27, 28]. Therefore, it is essential to examine the influence of such microenvironmental conditions (low glucose, low oxygen) when assessing the suitability of cell-based scaffold strategies to stimulate IVD tissue regeneration.

This work describes an innovative approach to fill defects of the AF using covalently cross-linked alginate porous scaffolds which exhibit shape-memory recovery characteristics. Porous biomaterial scaffolds with shape-memory properties have several advantages including the ability to be delivered to a defect site using minimally invasive surgical (MIS) approaches with the specific aim to provide a support template for AF cell proliferation and tissue formation. Mechanical properties of the freeze-dried scaffold can be tailored depending on cross-linker concentration, without impacting on the porous structure characteristics. More importantly, this scaffold was shown to facilitate immediate filling of an AF defect after injection in an *ex-vivo* IVD model. *In vitro* experiments demonstrated that scaffolds supported AF cell proliferation and matrix deposition when cultured under IVD-like microenvironmental conditions (low oxygen concentration and low glucose media).

2. Materials and methods

2.1. Fabrication of covalently cross-linked porous alginate scaffolds

Sodium alginate (alginate Pronova UP LVG) was purchased from FMC Biopolymer (Novamatrix, Sandvika, Norway) and all other chemicals were from Sigma-Aldrich (Arklow, Ireland). Alginate was covalently cross-linked using carbodiimide chemistry as previously described [29-31]. Briefly, alginate was dissolved in sterile morpholine ethanesulfonic acid buffer pH 6.0 (MES at 0.1 M) with NaCl at 0.2 M, to a final concentration of 3.3% and filtered using 0.45 µm filter (Sarstedt, Wexford, Ireland). Sterile solutions of and N-hydroxysuccinimide (NHS) and 1-ethyl-3-(dimethylaminopropyl) carbodiimide (EDC) prepared in MES buffer were added to alginate solution and homogenised for at least 5 min at a final molar ratio of 2:1:2 for EDC : NHS : COO^-. Finally, the bifunctional cross-linker (adipic acid dihydrazide (AAD)), was added to the reactive solution at different concentrations (expressed in % depending on n_{NH2} / n_{COOH}), quickly homogenised and cast in a mould. The cross-linking reaction was performed overnight at room temperature (R.T.) and

the slab of cross-linked alginate hydrogel was finally washed in deionized water for 72 hrs with frequent changes in order to remove any unreacted chemical reagents. Porous scaffolds were obtained using a freeze-drying process. The hydrogel slab was placed in a petri dish on the cooling shelf of a freeze-dryer (Labconco Triad™, Kansas City, MO USA), cooled at a constant cooling rate (1.0ºC/ min) to a desired final freezing temperature (T = -30ºC) to allow ice crystallization and finally sublimated under vacuum (0.2mBar) for 18 hrs at a temperature of -10°C to create the porous network. After the freeze-drying process, scaffolds of 4mm x 3mm (diameter x height) were created using a sterile biopsy punch.

2.2. Assessment of biomechanical properties

All constructs (cell-free and cell-laden, at day 0 and day 21 (n=3 for each group)) were mechanically tested in unconfined compression immersed in phosphate buffed saline (PBS) at R.T., using a standard materials testing machine with a 5N load cell (Zwick Z005, Roell, Germany) as previously described [32]. A preload of 0.01N was applied to ensure that the surfaces of the constructs were in direct contact with the impermeable loading platens. Stress relaxation tests were performed, consisting of a ramp and hold cycle with a ramp displacement of 1µm/s until 10% strain was obtained (the maximal stress recorded corresponding to the peak stress) and maintained until equilibrium was reached for at least 45 min. (corresponding to the equilibrium stress). The equilibrium modulus was calculated by taking the stress determined at complete relaxation (equilibrium) and dividing by the applied strain (10%) respectively.

Biopsies of AF tissue from IVDs obtained from bovine tails (5mm Ø x 3mm H) were tested in the axial direction (n=3) and compared to scaffold constructs.

2.3. Annulus fibrosus cell isolation and expansion

Intervertebral discs (IVDs) from the lumbar region were harvested from the spine of a single porcine donor (≈ 40 kg / 4 months old) within three hours of sacrifice. IVDs were carefully exposed and the AF tissue removed under aseptic conditions. Finely diced tissue was enzymatically digested in 2.5mg/ml pronase solution (Calbiochem, Merck Millipore, Darmstadt, Germany) for 1 hour followed by collagenase digestion at 1mg/mL (Invitrogen, Dublin, Ireland) at 37°C under constant rotation in serum free low glucose low-glucose Dulbecco's modified eagles medium (1mg/ml D-Glucose, 200mM L-Glutamine; LG-DMEM) containing antibiotic/antimycotics (100U/ml penicillin, 100µg/ml streptomycin). Digested tissue/cell suspension was passed through a 100µm cell strainer to remove tissue debris. Cells were then washed three times by repeated centrifugation at 650G for 5 mins. AF cells were plated at $5x10^3$ cells/cm^2 and expanded until passage 2 in T-175 flasks (Sarstedt, Wexford, Ireland) in LG-DMEM) supplemented with 10% foetal bovine serum (FBS), penicillin (100U/ml)-streptomycin (100µg/ml) (all GIBCO, Invitrogen, Dublin, Ireland), amphotericin B (0.25µg/ml, Sigma-Aldrich, Arklow, Ireland), and 5ng/ml Fibroblast Growth Factor-2 (FGF-2; ProSpec-Tany TechnoGene Ltd, Israel) at 37°C in a humid atmosphere containing 5% CO_2, with medium changed every 3-4 days.

2.4. Cell seeding on porous alginate scaffolds

Freeze-dried alginate scaffolds were fully compressed with a forceps and rehydrated with 100µL of AF cell suspension ($8x10^6$ cells/mL, corresponding to the natural cell density of AF tissue [33]). After seeding, scaffolds were maintained at 37°C in a humidified incubator for 2 hrs to allow cells to attach. Scaffold constructs were cultured in 24-well plates (Costar Corning, Amsterdam, The Netherlands) with 2mL of chemically defined medium (CDM) consisting of LG-DMEM supplemented with penicillin (100U/ml)-streptomycin (100µg/ml) (both GIBCO, Biosciences, Ireland), 100µg/ml sodium pyruvate, 40µg/ml L-proline, 50µg/ml

L-ascorbic acid-2-phosphate, 1.5mg/ml BSA, 1×insulin–transferrin–selenium, 100nM dexamethasone (all from Sigma-Aldrich, Ireland). Constructs were cultured in CDM supplemented with TGF-β3 at 10ng/mL (ProSpec-Tany TechnoGene Ltd, Israel; identified as group "+ TGF") compared to TGF-β3-free media (identified as group "- TGF") at 37ºC in either normoxic oxygen concentration (20% O_2) or low oxygen concentration (5% O_2) to mimic the microenvironment normally experienced *in vivo* [24, 33, 34] (n=6 for each group and condition). Media exchanges were performed twice weekly for the total culture duration of 21 days. Constructs were assessed at days 0 and 21 in terms of cell viability (n=1), biochemical content (n=3) and histologically (n=2).

2.5. Cell viability

At day 0 and day 21, cell viability was assessed using a LIVE/DEAD® viability/cytotoxicity assay kit (Invitrogen, Bio-science, Ireland). Briefly, constructs were cut in half, washed in PBS followed by incubation in PBS containing 2μM calcein AM (green fluorescence of membrane for live cells) and 4μM ethidium homodimer-1 (red fluorescence of DNA for dead cells; both from Cambridge Bioscience, UK). Sections were again washed in PBS, imaged at magnification x10 with an Olympus FV-1000 Point-Scanning Confocal Microscope (Southend-on-Sea, UK) at 515 and 615 nm channels and analysed using FV10-ASW 2.0 Viewer software. Z-stack images of 30 scans every 10μm in the cross-section of the scaffold were acquired for a total of 300μm depth.

2.6. Scanning Electron Microscope (SEM) examination and pore size measurement

Prior to Scanning Electron Microscope (SEM) observation, scaffolds were cut in half and fixed with 4% paraformaldehyde solution (PFA) in sodium cacodylate – barium chloride buffer overnight at 4ºC followed by repeated washings in PBS. Fixed samples were dehydrated through successive graded ethanol baths (10 to 100%) followed by critical point drying with CO_2. Scaffolds were then sputter coated with an approximate 10nm thick gold film, and examined by SEM (Tescan Mira FEG-SEM XMU, Libušina, Czech Republic) using a lens detector with a 5kV acceleration voltage at calibrated magnifications. Pore size determination of the different scaffolds was evaluated by measuring the diameter of 15 pores present in the cross-section of each scaffold (n=3 for each AAD concentration).

2.7. Quantitative biochemical analysis

To quantify the accumulation of biochemical constituents, constructs were digested with 125µg/mL papain in 0.1M sodium acetate, 5mM L-cysteine-HCl, 0.05M EDTA, pH 6.0 (all from Sigma-Aldrich) at 60°C under constant rotation for 18 hrs (n=3 for each group). DNA content of each sample was quantified using the Hoechst Bisbenzimide 33258 dye assay, with a calf thymus DNA standard. sGAG content was quantified using the dimethylmethylene blue dye-binding assay (DMMB, Blyscan, Biocolor Ltd., Carrickfergus, United Kingdom), with a chondroitin sulphate standard. Total collagen content was estimated by measuring the hydroxyproline content using trans-4-Hydroxy-L-proline standard stock solution at 1 mg/mL (Fluka, Ireland). Samples were hydrolysed at 110°C for 18 hrs in 38% HCl and assayed using a chloramine-T assay [35].

2.8. Histology and immunohistochemistry

Staining of matrix deposition in the scaffolds was performed after fixation, dehydration and wax embedding (n=2 for each group). Briefly, at the end of the culture period, constructs

were removed from the culture media, washed in PBS and fixed in 4% PFA solution in sodium cacodylate – barium chloride buffer overnight at 4ºC. After removing the fixative and washing, samples were gradually dehydrated through 70-100% ethanol series with a final xylene change, before embedding in wax. Sections of 8µm were obtained with a microtome (Leica RM2125RT, Ashbourne, Ireland) and affixed to microscope slides (Polylysine™, VWR, Dublin, Ireland). Prior to staining, sections were dewaxed and rehydrated in 100-70% ethanol baths followed by distilled water. Cellular colonization and matrix deposition was stained with haematoxylin and eosin (H&E), whereas sulphated-Glycosaminoglycan (sGAG) and collagen distribution were analysed histologically using Aldehyde Fuchsin - Alcian Blue and PicroSirius Red stains respectively.

Collagen types I and II were evaluated using a standard immunohistochemical technique. Briefly, sections were treated with peroxidase, followed by treatment with chondroitinase ABC (Sigma-Aldrich) in a humidified environment at 37°C to enhance permeability of the extracellular matrix. Sections were incubated with goat serum to block non-specific sites and collagen type I (ab6308, 1:400; 1mg/mL), collagen type II (ab3092, 1:100; 1mg/mL) primary antibodies (mouse monoclonal, Abcam, Cambridge, UK) were applied for 18 hrs at 4ºC. Next, the secondary antibody (Anti-Mouse IgG biotin conjugate, 1:200; 2.1mg/mL) (Sigma-Aldrich) was added for 1 hr followed by incubation with ABC reagent (Vectastain PK-400, Vector Labs, Peterborough, UK) for 45 min. Finally sections were developed with DAB peroxidase (Vector Labs) for 5 min. Slices were subsequently dehydrated and soaked in xylene before adding the mounting media (Vectamount mounting medium, Vector lab, H5000) and the sections were covered with a coverslip. Slides were observed using a microscope (Olympus BX41) at x10 magnification. Positive and negative controls were included in the immunohistochemistry staining protocol for each batch (*i.e.* ligament for collagen type I and cartilage for collagen type II). Collagen type I staining in control tissues

and background staining of the scaffolds at day 0 for histological analyses and for immunohistochemistry of collagen type I are presented in supplementary data 1 (SD1).

2.9. Statistical analysis

Statistical analyses were performed using GraphPad Prism (version 5) software with 3 samples analysed for each experimental group. One way ANOVA was used for analysis of variance with Bonferroni's post-tests to compare between groups. Results are reported as mean ± standard deviation. Significance was accepted at a level of $p < 0.05$.

3. Results

3.1. Fabrication and characterization of alginate porous scaffold

Covalent amide bonds between carboxyl groups present on alginate chains and amine groups on the bifunctional cross-linker (adipic acid dihydrazide, AAD) were created using carbodiimide chemistry. The evaluation of the equilibrium modulus of freeze-dried porous scaffolds demonstrated that the mechanical properties can be tailored depending on the concentration of AAD incorporated in the alginate solution prior to cross-linking (Fig. 1A). A high concentration of 45% of AAD allowed creating porous scaffold with the equilibrium modulus significantly higher than with low AAD concentrations of 5, 15 and 25%. No significant differences in pore size diameter were observed as a function of cross-linking density (Fig. 1B). Indeed, all of the scaffolds exhibited a highly interconnected porous cross-section with an average pore size of ≈ 300µm, as illustrated for the scaffold based on 45% AAD (Fig. 1C), using scanning electron microscopy (SEM). For all subsequent experiments, porous scaffolds obtained with 45% of AAD were used.

Alginate-based scaffold constructs obtained using the covalent cross-linking method demonstrated shape-memory properties (Fig. 2). Indeed, scaffolds with desirable sizes and shapes were created and were capable of being collapsed and restored to their initial geometry through simple rehydration (Fig. 2A). Scaffolds retained the initial geometry after rehydration within 15 seconds (Supplementary video 1). After compression, these scaffolds displayed a very high water uptake capability (> than 40mg of water / mg of scaffold, corresponding to a swelling capability of 4000%) (Fig. 2B) and can be repeatedly compressed and relaxed without damage (Fig. 2C). Finally, simulation of scaffold delivery into a defect created in the AF tissue of a bovine intervertebral disc (IVD) demonstrated that the scaffold (initial size of 5mm Ø x 3mm) can be compressed and introduced through the open end of a

20G catheter. After injection and rehydration, the scaffold completely filled the 5mm diameter and 5mm deep defect in the IVD (Fig. 2D).

3.2. *In vitro* cell viability and proliferation

AF cells were seeded on compressed scaffolds as illustrated in Fig. 2B. Rehydration of collapsed scaffolds with a cell suspension permitted homogenous cellular infiltration and distribution throughout the porous network of scaffold constructs. LIVE/DEAD® analysis (performed 18 hrs post-seeding) demonstrated the absence of toxic residue from the chemical reaction as no red fluorescence could be detected (data not shown). However, after 21 days of culture, major differences were observed in cell behaviour depending on TGF-β3 supplementation (Fig. 3). Indeed, in a TGF-free media, cells did not attach to the scaffold during the culture period but created small clusters, the number of which appeared to decrease overtime (Figs. 3A, B and C). In comparison, with TGF supplemented media, cells rapidly proliferated and invaded the porous scaffold (Figs. 3D, E and F). In this group, within a few days of seeding, some AF cells exhibited spindle-shape morphology and started to spread into the porous scaffold. After 21 days, higher cell activity in the "+ TGF" group could be denoted by the macroscopic appearance of the constructs, which were completely opaque (Fig. 3H), whereas the constructs in the "-TGF" group remained transparent with some isolated cell clusters (Fig. 3G).

Differences in cellular behaviour depending on TGF-β3 media supplementation and oxygen concentration were observed for both LIVE/DEAD® and SEM analysis (Fig. 4). Cell viability in TGF-free media remained relatively high (Figs. 4A and B) for both 5% and 20% oxygen conditions. Interestingly, without TGF-β3 supplementation cells agglomerated and formed clusters, but there was a difference in the size and in the number of clusters depending on oxygen concentration. Specifically, in TGF-free media, low oxygen concentration (O_2 at 5%, Fig. 4A) stimulated cell proliferation and increased the number of

clusters compared to normoxic oxygen conditions (O_2 at 20%, Fig. 4B). Moreover, SEM analysis also illustrated that the number of clusters and the number of cells per cluster were higher in low oxygen environment, as the size of the clusters seemed larger in this group (Figs. 4E and F). DNA quantification supported these observations (Fig. 4I), with the amount of DNA in scaffolds incubated at 5% O_2 being significantly higher than at 20% O_2. Nevertheless, for both groups ("- TGF" at 5% and 20% O_2), the DNA values were significantly lower compared to day 0. Supplementation with TGF-β3 had a strong effect on cellular proliferation and matrix deposition. LIVE/DEAD® analysis revealed that the addition of TGF-β3 stimulated scaffold colonization by AF cells. Moreover, SEM analysis revealed an abundant extra-cellular matrix (ECM) deposition secreted only when AF cells were stimulated by TGF-β3. This fibrous matrix completely filled the porous network of the scaffold, independent of the oxygen concentration (Figs. 4G and H).

In contrast to the positive effect of low oxygen concentration in "- TGF" group on cell proliferation as previously described, for TGF-β3 supplementation, cell viability and DNA content was higher at 20% O_2 concentration compared to 5% O_2 (Fig. 4I). This difference may be attributed to cell death, which appeared to be higher in 5% O_2 in comparison to 20% O_2 (Figs. 4C and D).

3.3. ECM deposition analyses in the scaffold

Having previously demonstrated that TGF-β3 supplementation was essential to stimulate ECM deposition by AF cells, only histological and immunohistochemical analyses for "+ TGF" groups is presented. By day 21, in supplemented media, complete scaffold colonization by AF cells occurred with clear evidence of matrix deposition throughout the scaffold as demonstrated by H&E staining (Figs. 5A, B and SD-2). Cell-seeded scaffolds exhibited an accumulation of clusters of high cell density throughout the porous network, which is

different compared to native AF tissue organization (Fig. 5C) where the cells are homogeneously distributed within the fibrous tissue. Histological staining of the ECM using Aldehyde Fuchsin - Alcian Blue confirmed intense deposition of sGAG in AF-seeded scaffolds subjected to both oxygen concentration conditions (Figs. 5D, E and SD-2B, E) compared to native AF tissue (Fig. 5F). Biochemical analysis revealed that total sGAG (expressed in µg/µg of DNA) was significantly higher in 5% O_2 compared to 20% O_2 culture conditions, and reached relatively similar values compared to native AF tissue for scaffolds maintained in hypoxic conditions (Fig. 5G).

ECM of AF-seeded scaffolds exhibited strong collagen staining for both 5% and 20% O_2 culture conditions (Figs. 6A, B) comparable to that of native AF tissue (Fig. 6C), and immunochemistry revealed an abundance of collagen type I, which is the major collagen characterizing the fibrous nature of AF tissue [36] (Figs. 6D, E and F). Minimal staining of collagen type II was detected in scaffolds at day 21 and in AF tissue (data not shown). Nevertheless, collagen accumulation, as determined through biochemical analysis of the hydroxyproline/DNA was significantly lower than in native AF tissue (factor of 10) for both oxygen concentrations (Fig. 6G). After 21 days, sGAG/HYP ratio ranged between 17 and 27 in "+TGF" group for 20% and 5% O_2 respectively, which was significantly higher than the calculated ratio of 3.1 for native AF tissue.

3.3. Influence of ECM deposition on the mechanical property of the constructs

TGF-β3 media supplementation had a direct effect on the mechanical properties of porous scaffold constructs. After 21 days of culture, "+ TGF" scaffold constructs exhibited stress relaxation profiles similar to that of native tissue, unlike the "- TGF" constructs that did not exhibit this behaviour (Fig. 7A). Due to (i) the absence of matrix in porous constructs without TGF supplementation ("- TGF" group), and due to (ii) the high elastic property of covalently

cross-linked alginate scaffolds; scaffolds from this group relaxed instantaneously during the initial compression ramp. Unsurprisingly, mechanical testing results for day 0 and for day 21 "- TGF" were almost similar (data not shown).

In terms of peak stress, "+TGF" scaffolds constructs demonstrated higher properties compared to "- TGF" constructs at day 21 (Fig. 7B). Oxygen concentration did not appear to influence mechanical properties. For equilibrium modulus, no significant differences were observed between groups regardless of TGF-β3 supplementation (Fig. 7C), and were significantly lower than native AF tissue. In terms of percentage relaxation, "+TGF" constructs exhibited similar levels compared to native tissue and were significantly higher than "-TGF" scaffolds (Fig. 7D).

4. Discussion

Due to injury or degeneration, increased biaxial circumferential tensile strains can develop in the AF tissue which can result in tears, fissures or herniation through which the soft gelatinous NP tissue can protrude and impinge on nerve roots resulting in pain and reduced disc height [7]. At present there are limited effective treatment strategies available to repair tears or fissures that may occur in the AF. Due to the poor intrinsic regeneration capability of this tissue there is significant interest in developing biomaterial scaffolds and cell-based strategies for biological regeneration and integration.

The aim of this work was to develop an alginate-based scaffold as a support template for AF cell proliferation and tissue formation, which could be administered to a defect site using minimally invasive surgical approaches. Alginate is a naturally occurring biomaterial which has been extensively investigated for IVD regeneration [37-39], but mainly as an ionically cross-linked hydrogel (using calcium salt, Ca^{2+}) for NP tissue regeneration. Unfortunately, due to (i) the poor mechanical stability, (ii) the difficulty to control *in situ*

gelation mechanism and (iii) the potential for tissue calcification; application of alginate-Ca^{2+} scaffold for AF regeneration is limited [30, 40]. One approach to overcome these limitations is to covalently cross-link the alginate chains using carbodiimide chemistry [29-31]. Shape-memory intrinsic properties of covalently cross-linked alginate scaffolds have previously been described as an injectable bulking agent for tissue engineering applications in terms of facilitating tissue ingrowth, inflammatory response and *in vivo* stability [29-31] but no evaluation for disc regeneration has been explored to date.

A key feature of shape-memory porous materials is the ability to reduce 3D scaffold volumes to less than 5% of the original volume [30]. The efficient restoration of the porous structure and rapid swelling potential of the shape-memory scaffolds also make them attractive materials for minimally invasive tissue repair, such as tears or fissures in the annulus fibrosus of the intervertebral disc. In this work, we have shown that alginate cross-linked with the bifunctional adipic acid dihydrazide cross-linker, followed by a freeze-drying step, permitted the fabrication of porous scaffolds suitable for IVD regeneration. *In vitro* experiments demonstrated that in the presence of TGF-β3 supplemented media, AF cells colonised the porous structure of scaffolds generating a matrix rich in sGAG and collagen throughout the scaffold volume. In contrast, in the absence of TGF-β3, cells agglomerated in small clusters with limited proliferation resulting in poor ECM deposition. It should be noted that it appears that cells did not directly attach to the alginate structure itself possibly due to the low cell adhesion properties of alginate which has previously been reported [41]. In the presence of TGF-β3, sufficient sGAG and collagen were deposited which enabled cell binding to this newly formed matrix. The dramatic influence of TGF-β3 media supplementation on cell proliferation and ECM deposition can be explained by the high expression of several anabolic growth factor receptors (*i.e.* transforming growth factor-β, fibroblast growth factor, insulin-like growth factor and bone morphogenic proteins) on NP and AF cells [42]. To stimulate

tissue ingrowth post-implantation, the fabrication of bioactive scaffolds through the incorporation or grafting of growth factors directly into/onto the biomaterial is pertinent and warrants further investigation.

An important factor that may limit the success of cell-based regeneration is the local microenvironment of the IVD. The lumbar IVDs are the largest avascular structures in the human body with the primary mode of nutrient delivery (e.g. oxygen, glucose) and metabolic waste removal (*e.g.* lactate) of the disc cells occurring by diffusion through the cartilage endplates or through blood vessels at the periphery of the annulus fibrosus. The IVD is therefore characterised by limited nutrition, high osmolarity, acidity, and low oxygen tension creating a challenging microenvironment [24, 27]. This hostile environment motivated the choice of low-glucose media and hypoxia conditions for our study. Recently, beneficial effects of low oxygen concentrations for maintaining chondrocyte-like phenotype of NP cells has been reported by Feng *et al.* [43], although, the same study did not demonstrate any significant beneficial effect of oxygen concentration on AF cellular behaviour. In contrast, we have shown in this study that in a TGF-β3 supplemented media, low oxygen tension significantly affected cell proliferation and viability. Other factors, such as serum and glucose deprivation, which are known to increase cell death in tissues with high cellular density [25, 44], combined with drastic hypoxic condition may explain these differences.

However, even if 5% O_2 is associated with increased cell death, our study showed that low oxygen concentration enhanced the sGAG/DNA ratio after 3 weeks of culture compared to 20% O_2. This second difference compared to the study of Feng *et al.* may be attributed to the different nature of the scaffold (nanofibrous poly-L-lactid scaffold) or the source of AF cells (from human herniated disc) [43]. As recently described, cells isolated from degenerated discs have been shown to secrete less sGAG compared to cells isolated from healthy IVDs [45]. In our experiment, sGAG/DNA ratio after three weeks of culture was similar to the

native non-degenerated IVD ratio, but collagen accumulation was significantly lower than native tissue control [45]. Previous attempts to recreate *in vitro* engineered composite-IVDs have shown that within three to four weeks of culture, the amount of collagen deposited corresponded to approximately 10% compared to native AF tissue, which is similar to that reported in this work. Longer culture or implantation periods may be required to accumulate significant amounts of ECM [46].

Mechanical property characterisation confirmed ECM deposition into the porous scaffolds. Indeed, for the "+ TGF" group, the stress-relaxation profile was similar to that of native AF tissue due to increase in matrix components, specifically sGAG content. In articular cartilage tissue, it is well established that sGAG contributes significantly to the compressive behaviour of the tissue [47]. However, we did observe differences mainly in equilibrium moduli during the relaxation phase, which can be attributed to the immaturity of the newly deposited ECM by AF cells (*i.e.* amount and organisation of collagen, interaction between the biomolecules of the ECM). This work assessed the unconfined compressive behaviour of the engineered tissues in a similar manner as previously described [48, 49]. Mechanical properties of annulus fibrosus tissue differs significantly between studies and may be a function of the testing protocol employed, species type [50], disease state [51] or age [52]. For example confined compression testing of porcine annulus fibrosus tissue resulted in an aggregate modulus of 51.84 ± 14.53kPa [53] which is significantly lower compared to that of bovine 0.74 ± 0.13 MPa [50] and healthy human tissue (0.56±0.21MPa) or degenerate human tissue (1.10±0.53MPa) [51]. In addition, Park et al. observed that the biomechanical properties of porcine annulus fibrosus tissue from lumbar discs changed significantly with increasing age (6.2 ± 1.3 to 44.0 ± 2.8 months old) becoming less flexible with slower relaxation behaviour under axial loading [52]. Our results showed that after 21

days of culture, "+ TGF" scaffold constructs exhibited stress relaxation profiles similar to that of native tissue, but the overall mechanical properties were lower than that of bovine annulus fibrosus tissue. Given the important function of the annulus fibrosus in resisting radial bulging during normal activity, the characterisation of the tensile properties of engineered tissues warrants further investigation.

The second important characteristic that strongly influences AF tissue mechanical properties is the arrangement and orientation of the collagen fibres. AF tissue displays anisotropic properties due to a high degree of structural arrangement of collagen type I fibres (associated with other minor collagens, such as type II, III, V VI, XII and XIV [36, 54]).

To mimic the natural orientation of collagen fibres in engineering scaffolds, various fabrication methods and specific architectures have been investigated such as porous sheets rolled into a concentric pattern [55], polymer meshes [46], microgrooves [56] or structures reinforced with nanofibers [57-59]. Such structures or architectures could potentially be incorporated into the alginate solution prior to cross-linking to create a composite alginate-based porous scaffold with aligned fibres. Nevertheless, further investigations would be required to evaluate the deliverability and the shape-memory characteristics of such composites. The advantage of the porous scaffolds developed in this work is that various geometries or sizes of scaffold can be created or simply cut to size and compressed into a very small volume before injection and expanded to fill irregular defects. Future experiments will be required to fully realise the suitability of these shape-memory alginate scaffolds to regenerate defects in AF using *ex-vivo* organ culture models in order to assess the integration and possible risks associated with implant migration during segment motion. Providing appropriate stability and integration of the implant after its insertion are significant prerequisites for clinical translation [60]. To address implant migration-related issues, we are

currently investigating possible solutions using different geometric configurations of porous scaffolds to facilitate retention in combination with biocompatible adhesives [11, 15, 61].

Due to the low cell density and limited vascular nature of AF tissue [33], migration of resident host AF cells into an acellular implanted scaffold with subsequent tissue ingrowth is expected to be slow and limited [62]. Therefore, the utilization of the porous scaffold as a vehicle for cell delivery is highly desirable. Another important consideration is how these porous scaffolds may perform in the harsh microenvironment of the IVD and if the infiltration of cytokines and macrophages in the immediate vicinity of an AF defect will promote or inhibit matrix formation [63]. However these important points can only be assessed through further *in vivo* experiments.

5. Conclusion

Porous shape-memory alginate scaffolds based on covalently cross-linked alginate were developed and characterised as a potential biomaterial for intervertebral disc regeneration. Scaffolds exhibited shape-memory capability suitable for delivery in annulus fibrosus defects of the IVD through minimal invasive approaches. *In vitro* experiments demonstrated that these porous scaffolds were cytocompatible when seeded with AF cells and supported cell penetration, proliferation and extra-cellular matrix deposition when cultured in IVD-like microenvironmental conditions (low oxygen and low glucose concentrations) with TGF-β3 media supplementation. After only three weeks of culture, sGAG and collagen type I were detected throughout the entire porous network of the alginate scaffold. The ability to deliver large size porous scaffolds using minimal invasive approaches that can potentially fill AF

defects and promote the regeneration of this tissue provides an exciting new avenue for disc repair.

6. Acknowledgment

This work was supported with resources/facilities of the Trinity Centre for Bioengineering and the MSc in Bioengineering programme. Furthermore, we would like to thank Dr. Gavin McManus (TBSI, School of Biochemistry and Immunology, Microscopy and Imaging Facility) and Neal Leddy (TCD, Centre for Microscopy and Analysis) for their technical assistance.

510

511 **Figure Legends**

512 **Fig. 1: Physical characterization of the porous scaffolds.** (A) Evaluation of the equilibrium
513 modulus and (B) pore size diameter of porous alginate scaffolds depending on the cross-
514 linker concentration (molar ratio in % of AAD compared to alginate in n_{NH2} /n_{COOH}). (C)
515 Scanning electron microscopy (SEM) illustration of the cross-section of alginate scaffold
516 cross-linked with 45% of AAD. Scale bar: C = 500µm. * indicates significance compared to
517 45% cross-linked alginate scaffold, $p<0.05$.

518

519 **Fig. 2: Illustration of the shape-memory characteristics of covalently cross-linked**
520 **porous alginate scaffolds.** Demonstration (A) of shape-memory properties of porous alginate
521 scaffolds (45% AAD), (B) of the deformation capability in dry state and rehydration with cell
522 suspension, and (C) of the elasticity of hydrated scaffolds. (D) *Ex-vivo* demonstration of the
523 delivery of the porous alginate scaffold followed by rehydration in a 5mm defect created in
524 AF tissue of a bovine caudal IVD. The scaffold is indicated by the white arrows and the white
525 dashed line circle delineates the scaffold position after rehydration. Scale bar: D= 1cm.

526

527 **Fig. 3: Influence of TGF-β3 media supplementation on cluster size and density in**
528 **scaffolds over 21 days of culture.** Microscopic observation of the seeded scaffolds after 7,
529 14 and 21 days of culture in 20% O_2 concentration in (A-C) TGF-β3 free media illustrating
530 the morphology and low density of cell clusters or (D-F) TGF-β3 supplemented media
531 showing increased density of cell clusters in porous scaffolds. (G, H) Macroscopic
532 illustrations of scaffolds at the end of the culture period with and without TGF- β3
533 supplementation. Scale bars: A-F= 250µm, G-H= 1mm.

534 **Fig. 4: Evaluation of the cell viability, matrix deposition and cell proliferation in porous**

535 **scaffolds at day 21 cultured at either 5% or 20% O_2 with or without TGF-β3**
536 **supplementation.** (A-D) LIVE/DEAD® staining showing viable cells in green and dead cells
537 in red (magnification x10) and (E-H) SEM images of corresponding scaffold cross-sections,
538 showing the cluster of cells (long white arrowheads) and the newly fibrous ECM (short white
539 arrowheads) in the alginate porous scaffold (**+** highlights the smooth strut material of the
540 alginate scaffold). (I) DNA content compared to day 0 levels. * indicates significance
541 compared to "-TGF" group for the same given oxygen concentration, & compared to 5% O2
542 concentration, $p < 0.05$. Scale bars: E-F= 20µm, G-H= 50µm.

543

544

545

546 **Fig. 5: Histological examination of the tissue formation in the scaffold and analysis of**
547 **the sulphated-glycosaminoglycan (sGAG) deposition compared to native AF tissue.** (A,
548 B and C) Histological staining of tissue deposition using Hematoxylin and Eosin
549 (magnification x10) and (D, E and F) sGAG using Aldehyde Fuchsin - Alcian Blue
550 (magnification x10) of scaffolds supplemented with TGF-β3 and cultured at either 5% or
551 20% O_2 concentration compared to native AF tissue (scale bars: 100µm). (G) Quantification
552 of sGAG/DNA in scaffolds at day 21 compared to native tissue. * indicates significance
553 compared to "-TGF" group for the same given oxygen concentration, $^{\&}$ compared to 5% O_2
554 concentration, $^{!}$ compared to native AF tissue, $p < 0.05$.

555

556 **Fig. 6: Histological examination and quantification of the collagen deposition in**
557 **scaffolds at day 21 compared to native AF tissue.** (A-C) Histological staining of collagen
558 deposition using PicroSirius Red (magnification x10) and (D-F) immunohistochemical
559 localization of collagen type I (magnification x10) of scaffolds supplemented with TGF-β3

and cultured at either 5% or 20% O_2 concentration compared to native AF tissue (scale bars: 100µm). (G) Quantification of hydroxyproline/DNA content in scaffolds at day 21 compared to native tissue. * indicates significance compared to "-TGF" group for the same given oxygen concentration, & compared to 5% O_2 concentration, ! compared to native AF tissue, $p < 0.05$.

Fig. 7: Mechanical characterization of porous scaffolds at day 21 cultured at either 5% or 20% O_2 with or without TGF-β3 supplementation compared to native AF tissue. (A) Representative stress-time curves illustrating relaxation behaviour after a preload force of 0.01N (corresponding to ≈ 0.5 kPa), (B) peak stress, (C) equilibrium modulus and (D) relaxation (%).* indicates significance compared to "-TGF" group for the same given oxygen concentration, & compared to 5% O_2 concentration, ! compared to native AF tissue, $p < 0.05$.

Supplementary Data 1: Immunohistological staining for collagen type I in (A) porcine ligament, (B) porcine cartilage and (C) AF seeded-alginate scaffold at day 0. (D-F) Background staining of AF seeded-alginate scaffold at day 0 for (D) Hematoxylin and Eosin, (E) Aldehyde Fuchsin - Alcian Blue , and (F) PicroSirius Red (magnification x20). Scale bars: 100µm.

Supplementary Data 2: Low magnification histological images of tissue deposition in scaffolds at day 21 for (A, D) Hematoxylin and Eosin, (B, E) sGAG using Aldehyde Fuchsin - Alcian Blue and (C, F) collagen deposition using PicroSirius Red in TGF-β3 supplemented media and cultured at either 5% O_2 (A, B and C) or 20% O_2 (D, E and F) concentration (magnification x2). Scale bars: 1 mm.

Supplementary Video 1: Demonstration of the shape-memory capability and rehydration in

584 PBS of covalently cross-linked alginate porous scaffolds (video is in real time).

7. References

[1] Whatley BR, Wen X. Intervertebral disc (IVD): Structure, degeneration, repair and regeneration. Materials Science and Engineering C 2012;32:61-77.

[2] Biyani A, Andersson GB. Low back pain: pathophysiology and management. J Am Acad Orthop Surg 2004;12:106-15.

[3] Martin MD, Boxell CM, Malone DG. Pathophysiology of lumbar disc degeneration: a review of the literature. Neurosurg Focus 2002;13:E1.

[4] Moore RJ, Latham JM, Vernon-Roberts B, Fraser RD. Does plate fixation prevent disc degeneration after a lateral anulus tear? Spine 1994;19:2787-90.

[5] Yorimitsu E, Chiba K, Toyama Y, Hirabayashi K. Long-term outcomes of standard discectomy for lumbar disc herniation: a follow-up study of more than 10 years. Spine 2001;26:652-7.

[6] Sherman J, Cauthen J, Schoenberg D, Burns M, Reaven NL, Griffith SL. Economic impact of improving outcomes of lumbar discectomy. Spine J 2010;10:108-16.

[7] DePalma MJ, Ketchum JM, Saullo TR, Laplante BL. Is the history of a surgical discectomy related to the source of chronic low back pain? Pain Physician 2012;15:E53-8.

[8] Bailey A, Araghi A, Blumenthal S, Huffmon GV. Prospective, Multicenter, Randomized, Controlled Study of Anular Repair in Lumbar Discectomy: Two-Year Follow-up. Spine 2013;38:1161-9.

[9] Trummer M, Eustacchio S, Barth M, Klassen PD, Stein S. Protecting facet joints post-lumbar discectomy: Barricaid annular closure device reduces risk of facet degeneration. Clin Neurol Neurosurg 2013;115:1440-5.

608 [10] Bron JL, Helder MN, Meisel HJ, Van Royen BJ, Smit TH. Repair, regenerative and
609 supportive therapies of the annulus fibrosus: achievements and challenges. Eur Spine J
610 2009;18:301-13.
611 [11] Heuer F, Ulrich S, Claes L, Wilke HJ. Biomechanical evaluation of conventional anulus
612 fibrosus closure methods required for nucleus replacement. Laboratory investigation. J
613 Neurosurg Spine 2008;9:307-13.
614 [12] Ledic D, Vilendecic M, Gorensek M, Varga P, Eustacchio S, Trummer M, et al.
615 Prospective controlled one-year clinical results on the intrinsic therapeutics Barricaid; a
616 device for closing defects in the anulus. Spine J 2007;7:123S-4S.
617 [13] Gantenbein-Ritter B, Sakai D. Biomaterials for Intervertebral Disc Regeneration. In:
618 Ducheyne P, Healy, K. E., Hutmacher, D., Grainger, D. W., Kirkpatrick, C. J., editor.
619 Comprehensive Biomaterials: Elsevier; 2011. p. 161-9.
620 [14] Richardson SM, Mobasheri A, Freemont AJ, Hoyland JA. Intervertebral disc biology,
621 degeneration and novel tissue engineering and regenerative medicine therapies. Histol
622 Histopathol 2007;22:1033-41.
623 [15] Blanquer SB, Sharifi S, Grijpma DW. Development of poly(trimethylene carbonate)
624 network implants for annulus fibrosus tissue engineering. J Appl Biomater Funct Mater
625 2012;10:177-84.
626 [16] Chang G, Kim HJ, Kaplan D, Vunjak-Novakovic G, Kandel RA. Porous silk scaffolds
627 can be used for tissue engineering annulus fibrosus. Eur Spine J 2007;16:1848-57.
628 [17] Wan Y, Feng G, Shen FH, Balian G, Laurencin CT, Li X. Novel biodegradable poly(1,8-
629 octanediol malate) for annulus fibrosus regeneration. Macromol Biosci 2007;7:1217-24.
630 [18] Nerurkar NL, Elliott DM, Mauck RL. Mechanics of oriented electrospun nanofibrous
631 scaffolds for annulus fibrosus tissue engineering. J Orthop Res 2007;25:1018-28.

[19] Shao X, Hunter CJ. Developing an alginate/chitosan hybrid fiber scaffold for annulus fibrosus cells. J Biomed Mater Res A 2007;82:701-10.

[20] Saad L, Spector M. Effects of collagen type on the behavior of adult canine annulus fibrosus cells in collagen-glycosaminoglycan scaffolds. J Biomed Mater Res A 2004;71:233-41.

[21] Sato M, Kikuchi M, Ishihara M, Ishihara M, Asazuma T, Kikuchi T, et al. Tissue engineering of the intervertebral disc with cultured annulus fibrosus cells using atelocollagen honeycomb-shaped scaffold with a membrane seal (ACHMS scaffold). Med Biol Eng Comput 2003;41:365-71.

[22] Li CH, Yew AY, Kimball JA, McBride DQ, Wang JC, Lu DC. Comparison of operating field sterility in open versus minimally invasive microdiscectomies of the lumbar spine. Surg Neurol Int 2013;4:S295-8.

[23] Spoor AB, Oner FC. Minimally invasive spine surgery in chronic low back pain patients. J Neurosurg Sci 2013;57:203-18.

[24] Bartels EM, Fairbank JC, Winlove CP, Urban JP. Oxygen and lactate concentrations measured in vivo in the intervertebral discs of patients with scoliosis and back pain. Spine 1998;23:1-7; discussion 8.

[25] Grunhagen T, Wilde G, Soukane DM, Shirazi-Adl SA, Urban JP. Nutrient supply and intervertebral disc metabolism. J Bone Joint Surg Am 2006;88 Suppl 2:30-5.

[26] Lee DC, Adams CS, Albert TJ, Shapiro IM, Evans SM, Koch CJ. In situ oxygen utilization in the rat intervertebral disc. J Anat 2007;210:294-303.

[27] Johnson WE, Stephan S, Roberts S. The influence of serum, glucose and oxygen on intervertebral disc cell growth in vitro: implications for degenerative disc disease. Arthritis Res Ther 2008;10:R46.

[28] Mwale F, Ciobanu I, Giannitsios D, Roughley P, Steffen T, Antoniou J. Effect of oxygen levels on proteoglycan synthesis by intervertebral disc cells. Spine 2011;36:E131-8.

[29] Lee KY, Rowley JA, Eiselt P, Moy EM, Bouhadir KH, Mooney DJ. Controlling Mechanical and Swelling Properties of Alginate Hydrogels Independently by Cross-Linker Type and Cross-Linking Density. Macromolecules 2000;33:4291-4.

[30] Thornton AJ, Alsberg E, Albertelli M, Mooney DJ. Shape-defining scaffolds for minimally invasive tissue engineering. Transplantation 2004;77:1798-803.

[31] Wang L, Shansky J, Borselli C, Mooney D, Vandenburgh H. Design and fabrication of a biodegradable, covalently crosslinked shape-memory alginate scaffold for cell and growth factor delivery. Tissue Eng Part A 2012;18:2000-7.

[32] Buckley CT, Thorpe SD, O'Brien FJ, Robinson AJ, Kelly DJ. The effect of concentration, thermal history and cell seeding density on the initial mechanical properties of agarose hydrogels. J Mech Behav Biomed Mater 2009;2:512-21.

[33] Maroudas A, Stockwell RA, Nachemson A, Urban J. Factors involved in the nutrition of the human lumbar intervertebral disc: cellularity and diffusion of glucose in vitro. J Anat 1975;120:113-30.

[34] Ishihara H, Urban JP. Effects of low oxygen concentrations and metabolic inhibitors on proteoglycan and protein synthesis rates in the intervertebral disc. J Orthop Res 1999;17:829-35.

[35] Kafienah W, Sims TJ. Biochemical methods for the analysis of tissue-engineered cartilage. Methods Mol Biol 2004;238:217-30.

[36] Cassidy JJ, Hiltner A, Baer E. Hierarchical structure of the intervertebral disc. Connect Tissue Res 1989;23:75-88.

679 [37] Bertolo A, Mehr M, Aebli N, Baur M, Ferguson SJ, Stoyanov JV. Influence of different
680 commercial scaffolds on the in vitro differentiation of human mesenchymal stem cells to
681 nucleus pulposus-like cells. Eur Spine J 2012;21 Suppl 6:S826-38.
682 [38] Bron JL, Vonk LA, Smit TH, Koenderink GH. Engineering alginate for intervertebral
683 disc repair. J Mech Behav Biomed Mater 2011;4:1196-205.
684 [39] Chiba K, Andersson GB, Masuda K, Thonar EJ. Metabolism of the extracellular matrix
685 formed by intervertebral disc cells cultured in alginate. Spine 1997;22:2885-93.
686 [40] Sun J, Huaping T. Alginate-Based Biomaterials for Regenerative Medicine Applications.
687 Materials 2013;6:1285-309.
688 [41] Smetana K, Jr. Cell biology of hydrogels. Biomaterials 1993;14:1046-50.
689 [42] Le Maitre CL, Richardson SM, Baird P, Freemont AJ, Hoyland JA. Expression of
690 receptors for putative anabolic growth factors in human intervertebral disc: implications for
691 repair and regeneration of the disc. J Pathol 2005;207:445-52.
692 [43] Feng G, Li L, Liu H, Song Y, Huang F, Tu C, et al. Hypoxia differentially regulates
693 human nucleus pulposus and annulus fibrosus cell extracellular matrix production in 3D
694 scaffolds. Osteoarthritis Cartilage 2013;21:582-8.
695 [44] Urban JP, Smith S, Fairbank JC. Nutrition of the intervertebral disc. Spine
696 2004;29:2700-9.
697 [45] Mwale F, Roughley P, Antoniou J. Distinction between the extracellular matrix of the
698 nucleus pulposus and hyaline cartilage: a requisite for tissue engineering of intervertebral
699 disc. Eur Cell Mater 2004;8:58-63; discussion -4.
700 [46] Mizuno H, Roy AK, Zaporojan V, Vacanti CA, Ueda M, Bonassar LJ. Biomechanical
701 and biochemical characterization of composite tissue-engineered intervertebral discs.
702 Biomaterials 2006;27:362-70.

[47] Canal Guterl C, Hung CT, Ateshian GA. Electrostatic and non-electrostatic contributions of proteoglycans to the compressive equilibrium modulus of bovine articular cartilage. Journal of biomechanics 2010;43:1343-50.

[48] Recuerda M, Cote SP, Villemure I, Perie D. Influence of experimental protocols on the mechanical properties of the intervertebral disc in unconfined compression. J Biomech Eng 2011;133:071006.

[49] Recuerda M, Perie D, Gilbert G, Beaudoin G. Assessment of mechanical properties of isolated bovine intervertebral discs from multi-parametric magnetic resonance imaging. BMC Musculoskelet Disord 2012;13:195.

[50] Perie D, Korda D, Iatridis JC. Confined compression experiments on bovine nucleus pulposus and annulus fibrosus: sensitivity of the experiment in the determination of compressive modulus and hydraulic permeability. Journal of biomechanics 2005;38:2164-71.

[51] Iatridis JC, Setton LA, Foster RJ, Rawlins BA, Weidenbaum M, Mow VC. Degeneration affects the anisotropic and nonlinear behaviors of human anulus fibrosus in compression. Journal of biomechanics 1998;31:535-44.

[52] Park C, Kim YJ, Lee CS, An K, Shin HJ, Lee CH, et al. An in vitro animal study of the biomechanical responses of anulus fibrosus with aging. Spine 2005;30:E259-65.

[53] Yao H, Justiz MA, Flagler D, Gu WY. Effects of swelling pressure and hydraulic permeability on dynamic compressive behavior of lumbar annulus fibrosus. Annals of biomedical engineering 2002;30:1234-41.

[54] Roughley PJ. Biology of intervertebral disc aging and degeneration: involvement of the extracellular matrix. Spine 2004;29:2691-9.

[55] Wan Y, Feng G, Shen FH, Laurencin CT, Li X. Biphasic scaffold for annulus fibrosus tissue regeneration. Biomaterials 2008;29:643-52.

[56] Johnson WE, Wootton A, El Haj A, Eisenstein SM, Curtis AS, Roberts S. Topographical guidance of intervertebral disc cell growth in vitro: towards the development of tissue repair strategies for the anulus fibrosus. Eur Spine J 2006;15 Suppl 3:S389-96.

[57] Bhattacharjee M, Miot S, Gorecka A, Singha K, Loparic M, Dickinson S, et al. Oriented lamellar silk fibrous scaffolds to drive cartilage matrix orientation: towards annulus fibrosus tissue engineering. Acta Biomater 2012;8:3313-25.

[58] Nerurkar NL, Baker BM, Sen S, Wible EE, Elliott DM, Mauck RL. Nanofibrous biologic laminates replicate the form and function of the annulus fibrosus. Nat Mater 2009;8:986-92.

[59] Vadala G, Mozetic P, Rainer A, Centola M, Loppini M, Trombetta M, et al. Bioactive electrospun scaffold for annulus fibrosus repair and regeneration. Eur Spine J 2012;21 Suppl 1:S20-6.

[60] Wilke HJ, Heuer F, Neidlinger-Wilke C, Claes L. Is a collagen scaffold for a tissue engineered nucleus replacement capable of restoring disc height and stability in an animal model? Eur Spine J 2006;15 Suppl 3:S433-8.

[61] Schek RM, Michalek AJ, Iatridis JC. Genipin-crosslinked fibrin hydrogels as a potential adhesive to augment intervertebral disc annulus repair. Eur Cell Mater 2011;21:373-83.

[62] Bron JL, Mulder HW, Vonk LA, Doulabi BZ, Oudhoff MJ, Smit TH. Migration of intervertebral disc cells into dense collagen scaffolds intended for functional replacement. J Mater Sci Mater Med 2012;23:813-21.

[63] Anderson JM, Rodriguez A, Chang DT. Foreign body reaction to biomaterials. Semin Immunol 2008;20:86-100.

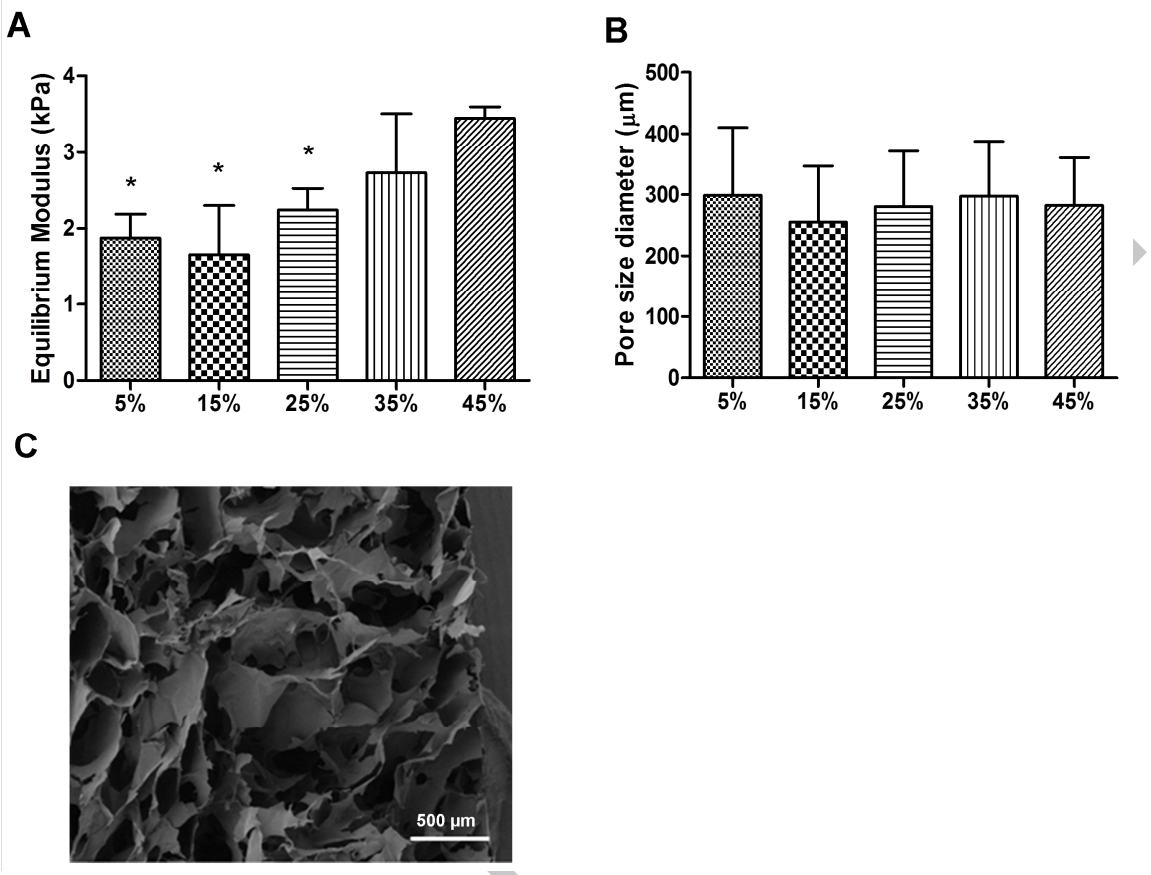

750

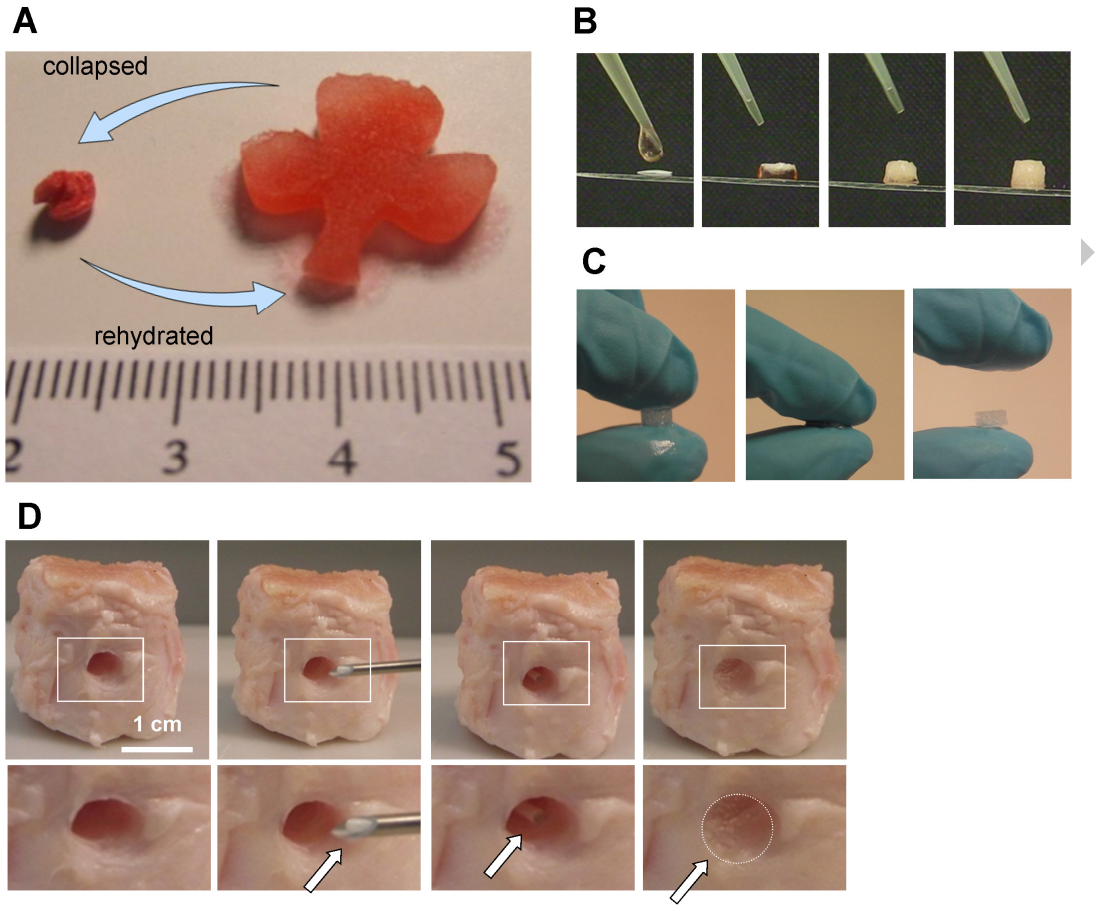

751

752

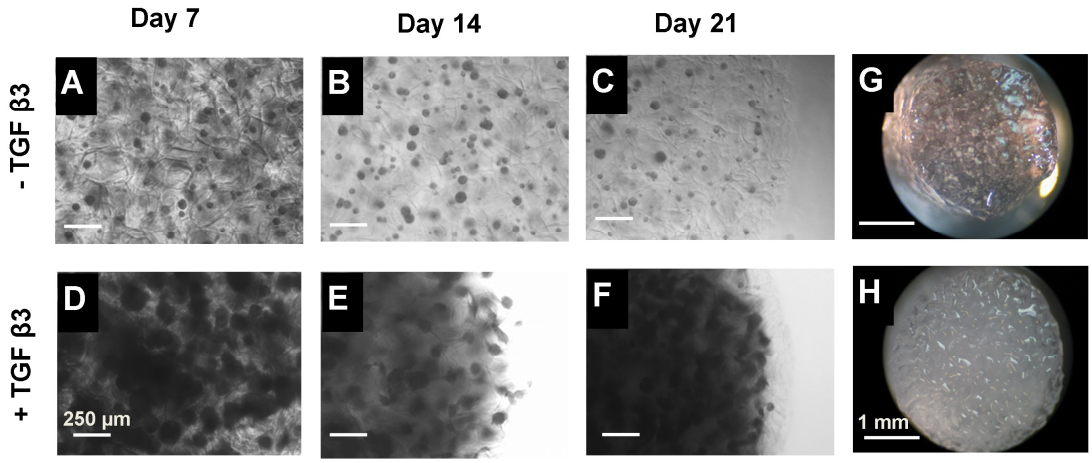

753

754

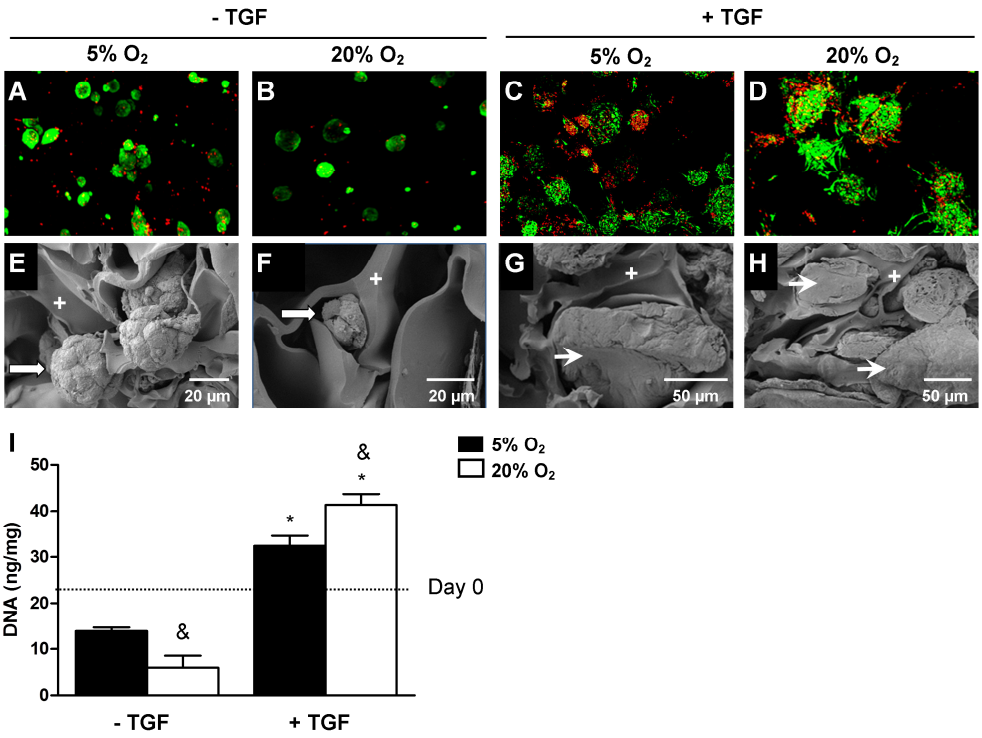

755

756

757

758

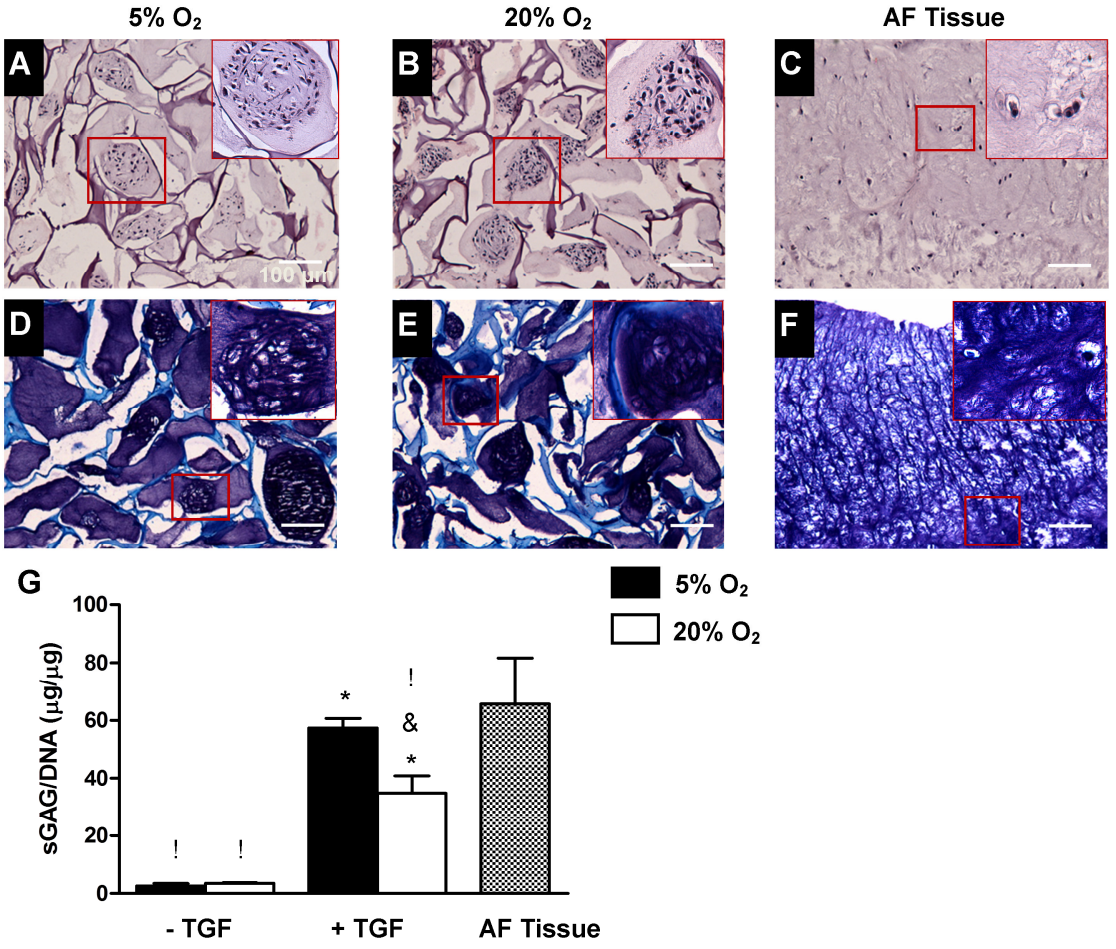

759

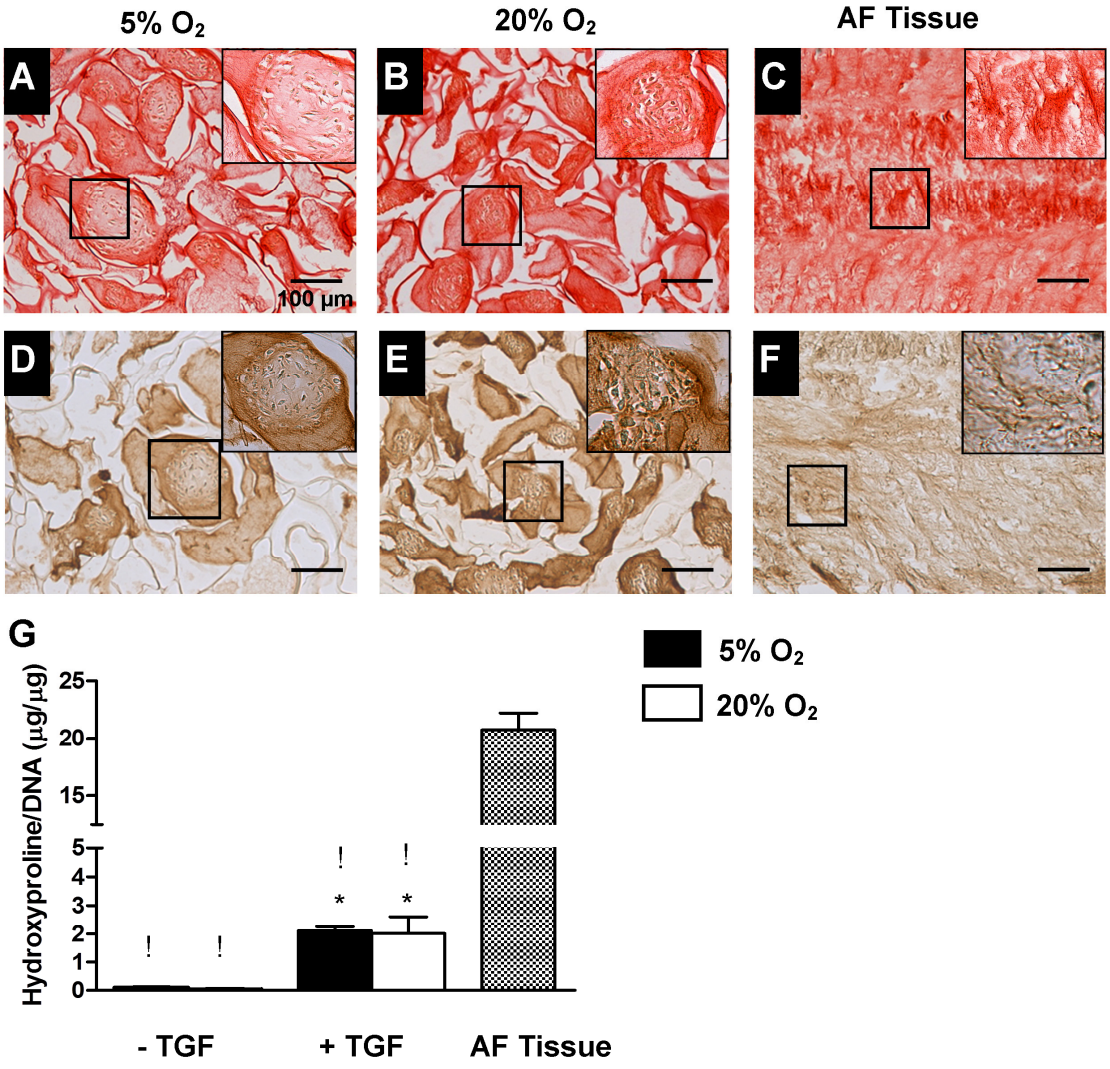

760

761

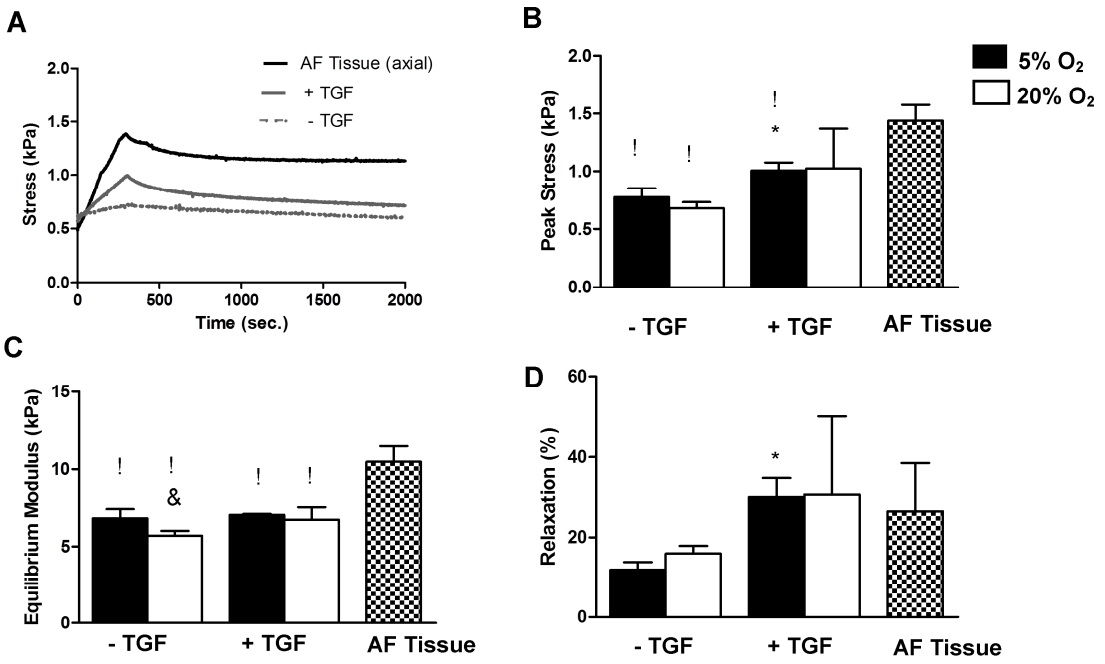

762

763

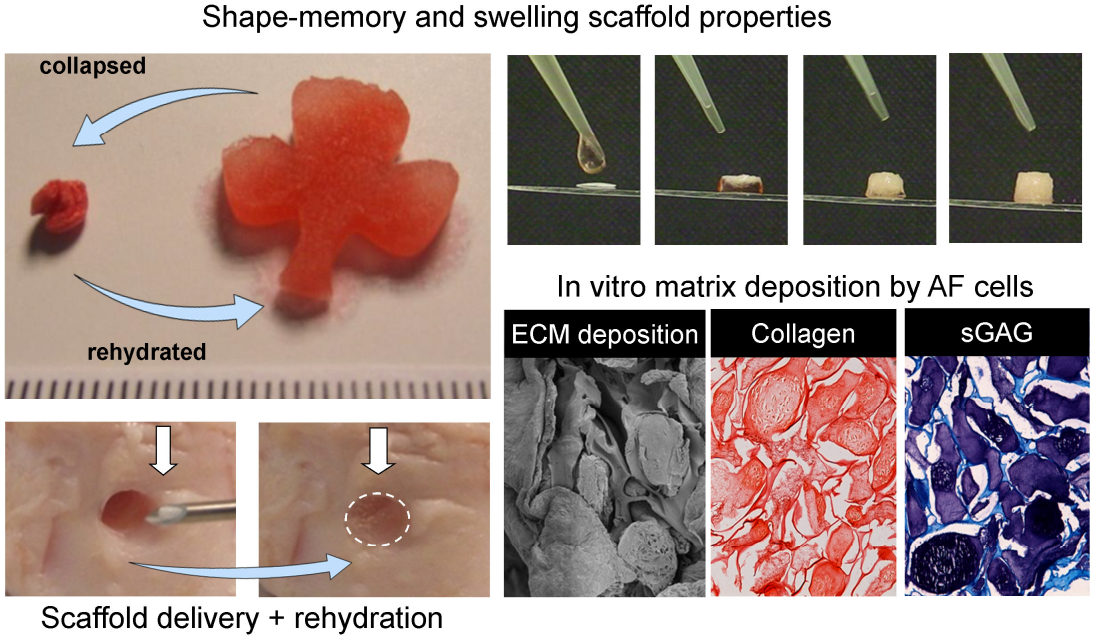

764

765

766 Graphical abstract

767

768